

Review

Implementation of a model of elastoviscoplastic consolidation behavior in Flac 3D

Verónica M. Giraldo Zapata*, Eduardo Botero Jaramillo, Alexandra Ossa Lopez

Instituto de Ingeniería, Universidad Nacional Autónoma de México (UNAM), Ciudad de México, Mexico

This paper call the model in Yin and Graham (1999) EVP3D (Yin call 3D EVP). The authors implemented Yin and Graham's EVP3D into commercial software named Flac3D which is the most popular finite difference software in the World.

ARTICLE INFO

Keywords:
Elastoviscoplastic
Finite difference
3D consolidation

ABSTRACT

The implementation of an **elastoviscoplastic three-dimensional model (EVP3D)** with the finite difference method is presented using the Flac3D analysis platform. This numerical model allows the time-dependent stress-strain behavior of soil to be studied while incorporating its viscous characteristics. An algorithm for solving the constitutive equations is developed and programmed using the centered finite difference method varying in time.

The historical case of the construction of Tarsuit Island in the Beaufort Sea in the Arctic Ocean is studied to calibrate and validate the model. A finite difference model that represents the construction stages is developed, and the short- and long-term behaviors are obtained. The model was calibrated and validated with the data record from an electric piezometer that was installed in the foundation of the artificial island, and the results of the algorithm are compared with the recorded data. The results are satisfactory and comparable to the measurements that were recorded for a year on the island, which demonstrates the applicability and validity of the model and its constitutive hypotheses.

1. Introduction

Traditional behavior models that have been developed for soft soils have mainly focused on the elasto-plastic component and neglected the viscous component. According to several researchers (e.g., [5,3,21,11,13]), in compressible soils such as clays, the deformation over time has a strong influence on the stress-strain behavior of soils; therefore, ignoring this effect can lead to unrealistic analysis. Some authors (e.g. Mesri (1975), Wehnert and Neher [23], Ovando [16], Gonzalez et al. [10]) have been reported evidence of elastoviscoplastic behavior of highly compressible clays.

The first elastoviscoplastic models were presented by Bjerrum [3], Adachi and Oka (1982), Leroueil et al. [13], Borja and Kavazanjian (1985) and **Yin and Graham [25]**, and they used different approaches for determining the time-dependent stress-strain behavior. This study involves the development of the elastoviscoplastic model in three dimensions (EVP3D) that was proposed by **Yin and Graham [28,29]**, which began with the one-dimensional model formulated by those authors in 1994 and 1996.

The EVP model referred to in this article is based on Perzyna's theory of viscoplasticity (1963) [17], the concept of instantaneous and delayed compression that was proposed by Bjerrum [3] and a new concept called the equivalent timeline, which represents the creep behavior of soil under the application of a constant load [26,27] and is

considered to be an extension of the Modified Cam Clay model that was defined by Roscoe and Burland [18]. The model was initially validated through triaxial tests on soil samples made with a mixture of Sand and Bentonite [28,29] getting good approximations between the numerical model and the laboratory test results.

In this study, we adopt the model proposed by [28,29] and the approach for generating a model coupled with the three-dimensional consolidation model proposed by Biot [2] to obtain the equations that relate the increase of excess pore pressure with the increasing volumetric deformations obtained from the EVP model [28,29]. Finally, the equations are solved using a finite difference scheme. Each of the constitutive equations from the coupled model is programmed in the Flac 3D platform to take advantage of the graphical interface and the storage capacity **in addition to the constitutive models that have been programmed.**

This is 3D Elastic Visco-Plastic Model by Yin and Graham (1999), called EVP3D in this paper.

2. Elastoviscoplastic model in **three dimensions (EVP3D)**

The EVP model, which was developed by Yin and Graham [28,29], is a model of soil behavior that involves two important aspects: the first is related to elastic behavior under a limited range of stresses, and the second is inelastic behavior that depends on the stress trajectories and time. Traditional geotechnical models are plastic models that do not include the influence of time; as such, they mainly depend on the

* Corresponding author.

E-mail address: vgiraldoz@ingen.unam.mx (V.M. Giraldo Zapata).

trajectories of the stresses to which the soil is subjected. However, some soils continue to deform when they are subjected to a constant stress state, which clearly shows that there is an additional component that many researchers attribute to the viscous properties of the material. The model used in this study involves these three aspects, which allows a greater approximation of the observed and measured soil behaviors. The model used in this study is an extension of the unidimensional model that was proposed by [26], which is based on the theory of one-dimensional consolidation under an isotropic state of stress. The development of the model requires concepts such as compressibility and soil deformability based on the approach proposed by Bjerrum [3], the classical plasticity theory from the viscoplasticity theory developed by Perzyna [17] and the Modified Cam Clay constitutive model that was proposed by Roscoe and Burland [18].

Numerous investigations have focused on one-dimensional analyses based on odometer deformation tests (e.g., [3,13,25,26]). However, Yin and Graham [28,29] extended the concept to three dimensions to determine the time-dependent stress-strain behavior of soils under triaxial and general states of stress. It is worth mentioned, that the study of engineering problems associated with tunnels, shafts, pipe jacking among others, requires tridimensional time-dependent stress-strain analyses to adequately represent soil behavior and its effects on such structures.

In addition to considering the concepts described above, the elastoviscoplastic model [28,29] modifies the timeline concept that was established by Bjerrum [3], which defines new concepts such as an equivalent timeline, instant timeline, and reference timeline. In addition, it considers an elliptical creep surface and the failure criterion of Von Mises (1913); thus, this model can be considered an extension of the Modified Cam Clay model of Roscoe and Burland [18].

The one dimensional elastoviscoplastic model that was proposed by Yin and Graham [26] is the basis of the EVP3D model of Yin and Graham [28,29]. The main difference between this model and the three-dimensional model is that the latter is given in terms of the isotropic stress (p') and not in terms of the effective vertical stress (σ_v), which differs substantially from the one-dimensional consolidation model.

Concepts such as the equivalent timeline, instant timeline and reference timeline, which are all represented in the ϵ_v : p' plane, are taken from the one-dimensional EVP model [26,27]. The equivalent timeline (t_e) is a parameter that allows the increase in soil deformation ($\dot{\epsilon}$) to be quantified (Fig. 1):

The volumetric strain at any point in Fig. 1 at a stress p'_m and for a known equivalent time t_e is defined as:

$$\epsilon_{vm} = \epsilon_{vm}^{ep} + \epsilon_{vm}^{vp} = \epsilon_{vm0}^{ep} + \frac{\lambda}{V} \ln \left(\frac{p'_m}{p'_{m0}} \right) + \frac{\psi}{V} \ln \left(\frac{t_0 + t_e}{t_0} \right) \quad (1)$$

Based on these concepts, the general equation of the EVP 1D model for

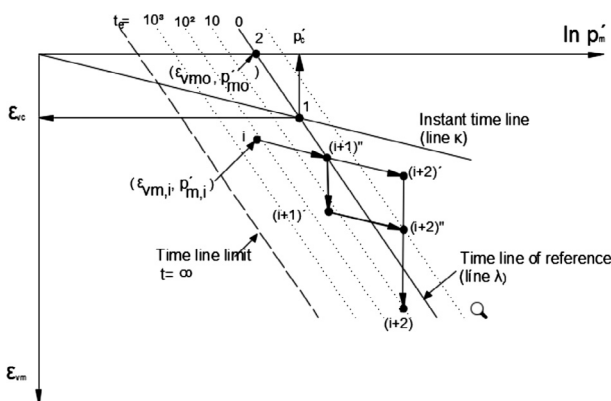


Fig. 1. Equivalent timeline, instant timeline, and reference timeline.

This figure is 100% from Yin and Graham (1999). "Equivalent time lime", "instant time line", and "reference time line" are all basic concepts and proposed by Yin and Graham (1989, 1994, 1999).

an isotropic stress state (Eq. (2)) is defined in terms of the total strain increment as the sum of the increase in elastic strain and the increase in creep strain:

$$\frac{\partial \epsilon_{vm}}{\partial t} = \frac{\kappa}{V p'_{m0}} \frac{d p'_m}{dt} + \frac{\psi}{V t_0} \exp \left[-(\epsilon_{vm} - \epsilon_{vm0}^{ep}) \frac{V}{\psi} \right] \left(\frac{p'_m}{p'_{m0}} \right)^{\frac{\lambda}{\psi}} \quad (2)$$

The EVP3D model [28,29] is based on several concepts, including the effect of time on the compressibility that was proposed by Bjerrum [3], the concept of soil creep that was proposed by Tresca (1869), Von Mises (1913), and Graham, Noonan and Lew (1983), the definitions of instantaneous and delayed deformations that were proposed by Bjerrum [3], Perzyna [17], the Modified Cam Clay model by Roscoe and Burland [18], and the one-dimensional elastoviscoplastic model that was developed by Yin and Graham [26]. The different theories and concepts allow a method to be defined to determine the total strain rate for normally consolidated soft soils to slightly overconsolidated soils in three-dimensional space.

According to the Modified Cam Clay model, the plastic potential g is equal to the flow surface function f , which depends on the level of effort and the history of soil hardening:

$$g = f(\sigma'_{ij}, k) = p'^2 - p' p'_m + \frac{q^2}{M^2} = 0 \quad (3)$$

where p'_m is the average effective isotropic stress at which the shear stresses q are equal to zero. In a general stress state, the average effective stress is $p' = (\sigma_{xx} + \sigma_{yy} + \sigma_{zz})/3$, and the generalized deviatoric stress $q = (3/2 S_{ij} S_{ij})^{1/2}$ for a triaxial stress state is $p' = (\sigma'_1 + 2\sigma'_3)/3$ and $q = \sigma_1 - \sigma_3$.

In this model, a logarithmic function is adopted to describe the creep behavior of the soil given that the strains approach infinity with infinite time; this is acceptable for the design life of geotechnical construction projects [28,29], which is considered to be greater than 50 years. According to the theory of viscoplasticity that was proposed by Perzyna (1963) [17], the viscoplastic strain rate $\dot{\epsilon}_{ij}^{vp}$ is calculated based on the flow rule:

$$\dot{\epsilon}_{ij}^{vp} = \gamma(\phi(f)) \frac{\partial g}{\partial \sigma'_{ij}} = S \frac{\partial g}{\partial \sigma'_{ij}} \quad (4)$$

where γ is related to the fluidity parameter, ϕ is a function of f , S is the scale function and is related to the flow surface (Zienkiewicz and Cormeau, 1974; Adachi and Oka, 1982; [8]; Kutter and Santhialingman, 1992; Borja and Kavazanjian, 1985; Yin and Graham [28,29]), g is the plastic potential function, and σ'_{ij} corresponds to the stress tensor.

The elastoviscoplastic model hypothesizes that the strain rate is constant at the creep surface, and thus the scale function S of Eq. (4) is derived. Considering a triaxial stress state, the following expressions are obtained:

$$\dot{\epsilon}_v^{vp} = \frac{\partial F}{\partial p'} = S(2p' - p'_m) \quad (5)$$

$$\dot{\epsilon}_s^{vp} = \frac{\partial F}{\partial q} = S \frac{2q}{M^2} \quad (6)$$

where $\dot{\epsilon}_v^{vp}$ is the volumetric viscoplastic strain rate, and $\dot{\epsilon}_s^{vp}$ is the viscoplastic deviatoric strain rate.

If the stress state (p' , q) is known, the mean isotropic stress p'_m is determined with Eq. (7), which expresses the soil consistency based on the theory of viscoplasticity:

$$p'_m = p' + \frac{q^2}{p' M^2} \quad (7)$$

Yin and Graham [28,29] hypothesized in the formulation of the EVP3D model that the volumetric viscoplastic strain rate is constant at the flow surface and is equal to the rate of volumetric strain under isotropic stress conditions ($q = 0, p' = p'_m$). Thus:

$$\dot{\epsilon}_{vm}^{vp} = \frac{\psi/V}{t_0} \exp \left[-(\epsilon_{vm} - \epsilon_{vm0}^{ep}) \frac{V}{\psi} \right] \left(\frac{p'_m}{p'_{m0}} \right)^{\frac{\lambda}{\psi}} \quad (8)$$

and assuming that $\dot{\epsilon}_v^{vp} = \dot{\epsilon}_{vm}^{vp}$, the scale function S is established, which is determined by:

$$S = \frac{\psi/V}{t_0} \exp \left[-(\epsilon_{vm} - \epsilon_{vm0}^{ep}) \frac{V}{\psi} \right] \left(\frac{p'_m}{p'_{m0}} \right)^{\frac{\lambda}{\psi}} \left(\frac{1}{2p' - p'_m} \right) \quad (9)$$

Based on these concepts, Yin and Graham [28,29] defined the constitutive equations of the elastoviscoplastic model in three dimensions using the following equations:

$$\dot{\epsilon}_v = \frac{1}{K^e} \dot{p}' + S(2p' - p'_m) \quad (10)$$

$$\dot{\epsilon}_s = \frac{1}{3G^e} \dot{q} + S \frac{2q}{M^2} \quad (11)$$

where K^e and G^e are the moduli for elastic component, that describe the non-linear elastic behavior of soil. K^e is the elastic bulk modulus and depends on the mean effective stress p' , and G^e is the elastic shear modulus and depends on K^e .

2.1. EVP3D model coupled with the general theory of three-dimensional consolidation

Based on the general theory of three-dimensional consolidation [2], Yin and Zhu (1999) transformed the EVP3D model into a coupled model, from which we obtain a set of equations to predict the soil behavior with time.

From this coupled model, we propose the first equation for the EVP3D model in terms of the excess pore pressure U :

$$\frac{\partial U}{\partial t} = K^e * \frac{k}{\gamma_w} * \left(\frac{\partial^2 U}{\partial x^2} + \frac{\partial^2 U}{\partial y^2} + \frac{\partial^2 U}{\partial z^2} \right) + K^e * S * (2p' - p'_m) \quad (12)$$

where k is a coefficient of permeability, γ_w is the volumetric weight of water (9.8 kN/m³)

To solve the EVP3D model, it is necessary to determine the increase in the volumetric isotropic strain $\dot{\epsilon}_{vm}$ based on the equation of the EVP 1D model, which is similar to the law of hardening in the Cam Clay model (Eq. (13)):

$$\dot{\epsilon}_{vm} = \frac{\kappa}{Vp'} \frac{dp'_m}{dt} + \frac{\psi}{Vt_0} \exp \left[\left(\epsilon_{vm0}^{ep} + \frac{\lambda}{V} \ln \left(\frac{p'_m}{p'_{m0}} \right) - \epsilon_{vm} \right) \frac{V}{\psi} \right] \quad (13)$$

where κ/V is an elastic parameter which represents the slope of the instantaneous line, λ/V , ϵ_{vm0}^{ep} and p'_{m0} are elastic-plastic parameters, and ψ/V and t_0 are creep parameters

The remaining equations correspond to Eqs. (10) and (11):

$$\dot{\epsilon}_v = \frac{1}{K^e} \frac{dp'}{dt} + \frac{\psi}{Vt_0} \exp \left[\left(\epsilon_{vm0}^{ep} + \frac{\lambda}{V} \ln \left(\frac{p'_m}{p'_{m0}} \right) - \epsilon_{vm} \right) \frac{V}{\psi} \right] \quad (14)$$

$$\dot{\epsilon}_q = \frac{1}{3G^e} \frac{dq}{dt} + \frac{\psi}{Vt_0} \exp \left[-(\epsilon_{vm} - \epsilon_{vm0}^{ep}) \frac{V}{\psi} \right] \left(\frac{p'_m}{p'_{m0}} \right)^{\frac{\lambda}{\psi}} \frac{2q}{M^2(2p' - p'_m)} \quad (15)$$

Eqs. (12)–(15) are the constitutive equations of the coupled EVP3D model.

3. Numerical solution of the coupled EVP3D model in the Flac 3D program

The explicit finite difference scheme is used to solve the first- and second-order differential equations that make up the coupled EVP3D model. Based on the initial and boundary conditions of the analyzed problem, this scheme obtains the spatial (x, y, z) and temporal (t)

variations of the group of variables that describe their behavior. This solution was incorporated into an algorithm that was developed in the FISH programming language [12]. This algorithm allows the behavior of continuous three-dimensional media that reach equilibrium and/or a continuous plastic flow to be modeled.

3.1. Numerical solution of the EVP3D model using the centered finite difference scheme

Eqs. (12)–(15) form a system of differential equations that can be represented through an explicit finite difference scheme, which is presented in the following subsections.

The nomenclature used in the resulting equations when applying the finite difference method is given below:

$$A_{ij,l}^n \quad (16)$$

where A is the variable of interest, n represents the time step, i is the step in the x axis, j is the step in the y axis, and l is the step in the z axis.

$$U_{ij,l}^{n+1} = \Delta t * S * K^e * (2p'^n_{ij,l} - (p'_m)^n_{ij,l}) + K^e * \frac{k}{\gamma_w} * \Delta t * [A + B + C] + U_{ij,l}^n \quad (17)$$

where

$$A = \frac{U_{i+1,j,l}^n - 2U_{ij,l}^n + U_{i-1,j,l}^n}{\Delta x^2}$$

$$B = \frac{U_{ij,l+1}^n - 2U_{ij,l}^n + U_{ij,l-1}^n}{\Delta y^2}$$

$$C = \frac{U_{ij,l+1}^n - 2U_{ij,l}^n + U_{ij,l-1}^n}{\Delta z^2}$$

$$(\epsilon_{vm})_{ij,l}^{n+1} = \Delta t \left[\frac{\kappa}{Vp'_m} \frac{(p'_m)^{n+1}_{ij,l} - (p'_m)^n_{ij,l}}{\Delta t} \right] + \Delta t \left\{ \frac{\psi}{Vt_0} \exp \left[-((\epsilon_{vm})_{ij,l}^n - \epsilon_{vm0}^{ep}) \frac{V}{\psi} \right] \left(\frac{(p'_m)^n_{ij,l}}{p'_{m0}} \right) \right\} + (\epsilon_{vm})_{ij,l}^n \quad (18)$$

where

$$(p'_m)_{ij,l}^{n+1} = p'^{n+1}_{ij,l} + \frac{q_{ij,l}^{n+1}}{p'^{n+1}_{ij,l} M^2}$$

$$p'^{n+1}_{ij,l} = p'^n_{ij,l} + \Delta u$$

$$(\epsilon_v)_{ij,l}^{n+1} = \Delta t \left[\frac{\kappa}{V(p'_m)^n_{ij,l}} \frac{(p'_m)^{n+1}_{ij,l} - (p'_m)^n_{ij,l}}{\Delta t} \right] + \Delta t \left\{ \frac{\psi}{Vt_0} \exp \left[-((\epsilon_{vm})_{ij,l}^n - \epsilon_{vm0}^{ep}) \frac{V}{\psi} \right] \left(\frac{(p'_m)^n_{ij,l}}{p'_{m0}} \right) \right\} + (\epsilon_v)_{ij,l}^n \quad (19)$$

$$(\epsilon_q)_{ij,l}^{n+1} = \Delta t \frac{1}{3G^e} q + \Delta t \left\{ \frac{\psi}{Vt_0} \exp \left[-((\epsilon_{vm})_{ij,l}^n - \epsilon_{vm0}^{ep}) \frac{V}{\psi} \right] \left(\frac{(p'_m)^n_{ij,l}}{p'_{m0}} \right)^{\frac{\lambda}{\psi}} \frac{2q}{M^2(2p'^n_{ij,l} - (p'_m)^n_{ij,l})} \right\} + (\epsilon_q)_{ij,l}^n \quad (20)$$

3.2. Stability of the finite difference method

Because the solution scheme for the equations that describe the EVP3D model is an explicit scheme, it is necessary to guarantee its convergence and stability. The condition that relates the spatial variation over time is known as the Courant-Friedrichs-Lewy condition [7], and it defines a critical value. Therefore, to obtain a numerical solution to the second-order differential equation (Eq. (17)) that governs the three-dimensional consolidation phenomenon in the EVP3D model, the following condition must be satisfied:

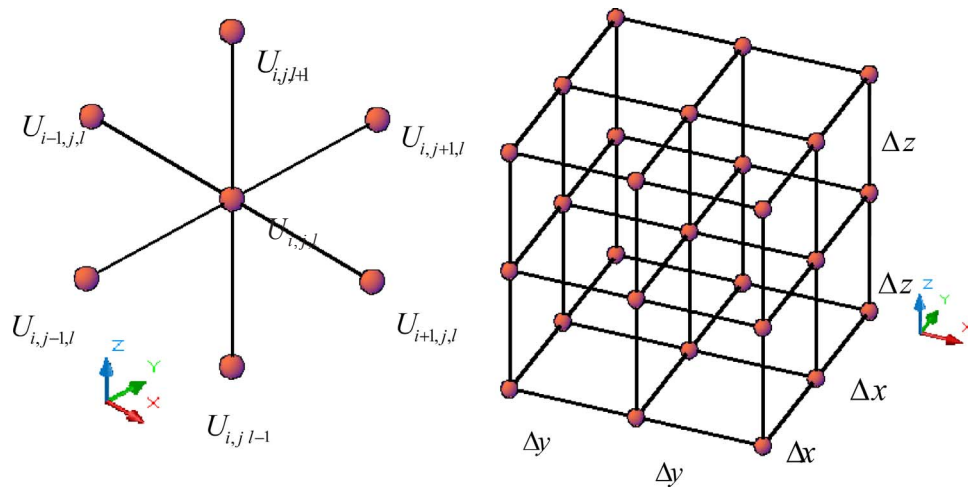


Fig. 2. Regular mesh for the three-dimensional finite difference solution.

$$C = \frac{C_v \Delta t}{(\Delta_{espacial})^2} \leq 0.5 \tag{21}$$

where C_v is the consolidation coefficient (L^2/T), Δt is the time step (T), and $\Delta_{espacial}$ corresponds to the smallest dimension of the mesh in the three spatial dimensions (Δx , Δy , Δz). If this condition is fulfilled, the spatial and temporal steps of the numerical modeling will be adequately determined to guarantee the convergence of the explicit method [24]. These characteristics for the particular case of the analysis are discussed in Section 4.

3.3. Mesh simplification

The centered finite difference scheme proposes the solution of the problem of rectangular meshes. In the three-dimensional case, the region around each central node is formed by six neighbors ($U_{i+1,j,l}$, $U_{i-1,j,l}$, $U_{i,j,l+1}$, $U_{i,j,l-1}$, $U_{i,j,l+1}$, $U_{i,j,l-1}$), two for each axis, and the pitch in each direction must be the same (Fig. 2). Two schemes for the regular mesh are presented in Fig. 2. In the first, the neighboring nodes are connected to a particular node, whereas in the second, several elements are connected to a particular node.

However, it is common for finite-difference algorithms to represent complex geometries by discretizing the continuous medium using regular and irregular meshes (more than six neighbors connected to a node) (Fig. 3). To avoid detracting from the applicability of the method

to complex or detailed geometries, it is necessary to transform irregular meshes into regular meshes. Therefore, a mechanism was implemented to transform irregular meshes into regular rectangular meshes using the Inverse Distance Weighted Interpolation (IDW) method. The IDW method is a deterministic method that is used for the multivariate interpolation of a dispersed set of known data. The main hypothesis is that every point in the data set of a continuous medium is related to the entire data set but is influenced more by the closest points; the value of a variable at a non-sampled point is the weighted average of known values in its vicinity (Lu and Wong, 2008). This allows the values at unknown points to be determined from the values n at a dispersed set of known points.

The equations for IDW interpolation are as follows:

$$U_p = \sum_{i=1}^n w_i U_i \tag{22}$$

$$w_i = \frac{d_i^{-\alpha}}{\sum_{i=1}^n d_i^{-\alpha}} \tag{23}$$

where U_p is the point where the value is unknown, U_i represents the values of the known points, n is the number of data points, d_i represents the distance from the unknown point to each of the known points, and α is a control parameter. According to Lu and Wong (2008), $\alpha = 2$. Fig. 4 shows a schematic of the IDW interpolation method, which indicates

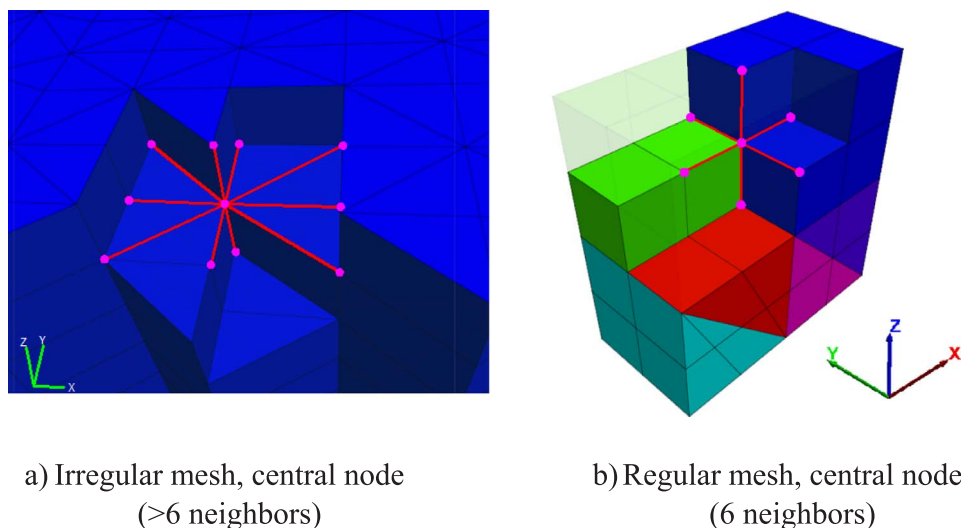


Fig. 3. Regular and irregular meshes.

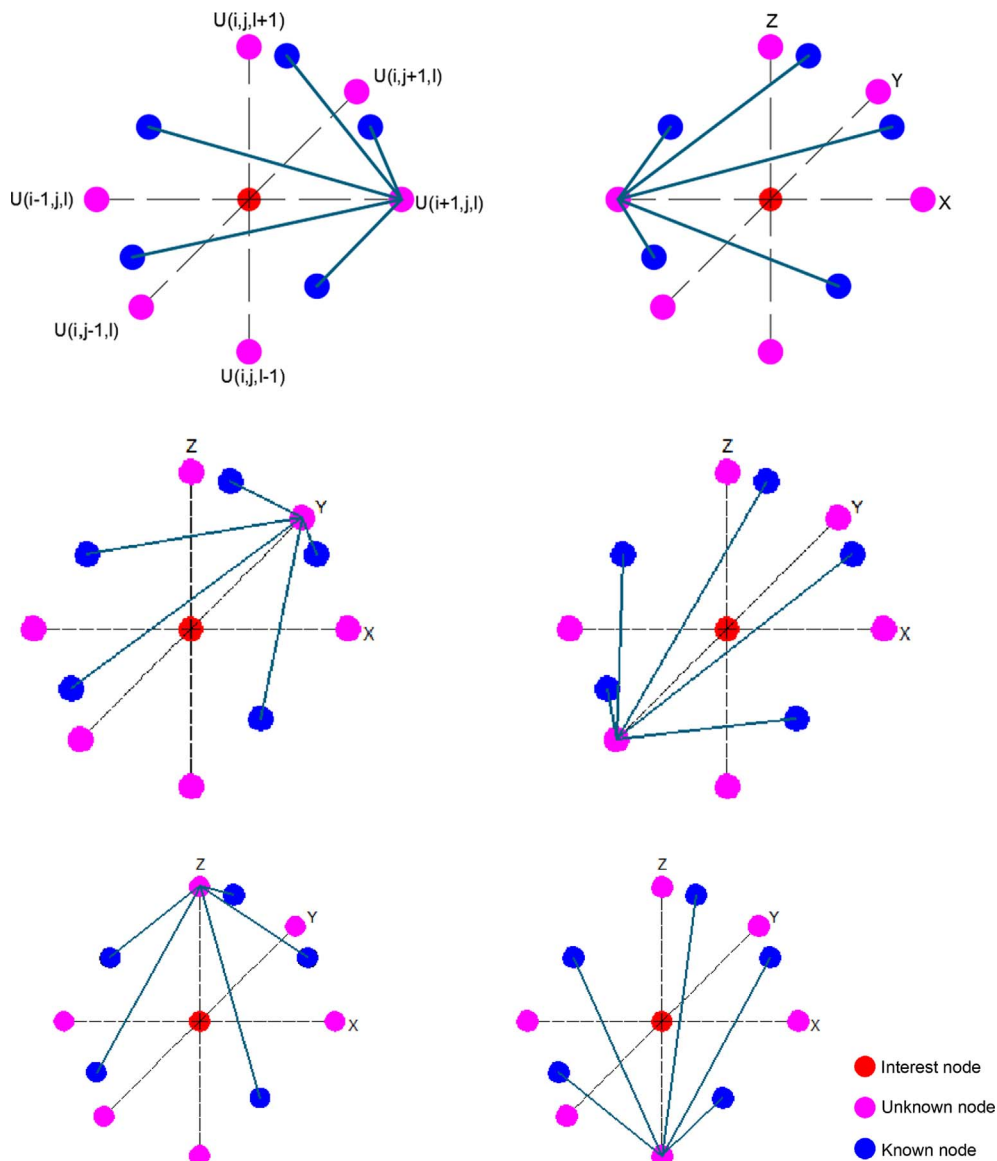


Fig. 4. Interpolation via the inverse weighted distance (IDW) method.

that the value of each unknown or virtual node is determined from the cloud of known nodes. In this way, a regular mesh is constructed, which can be solved with the centered finite difference method.

3.4. Algorithm developed to implement the EVP3D model

Next, a general description of the algorithm that was developed for the analysis of a three-dimensional continuous medium using the EVP3D model is presented.

To determine the geometry of the model, the mesh is generated following the mesh generation logic of the program used. The geometry must be continuous, and the elements that make up the model must have appropriate aspect ratios to enable convergence, stability, precision, and speed in the calculation.

The initial equilibrium conditions must be determined to establish the geostatic (stress state) and hydrostatic (pore pressure) conditions at the beginning of the stage to be evaluated.

The soil parameters necessary to execute the EVP3D model and the time interval to be evaluated are presented in equations (17)–(20).

To simplify the mesh simplification process, the conversion of irregular to regular meshes is performed by creating virtual nodes using

the IDW interpolation method.

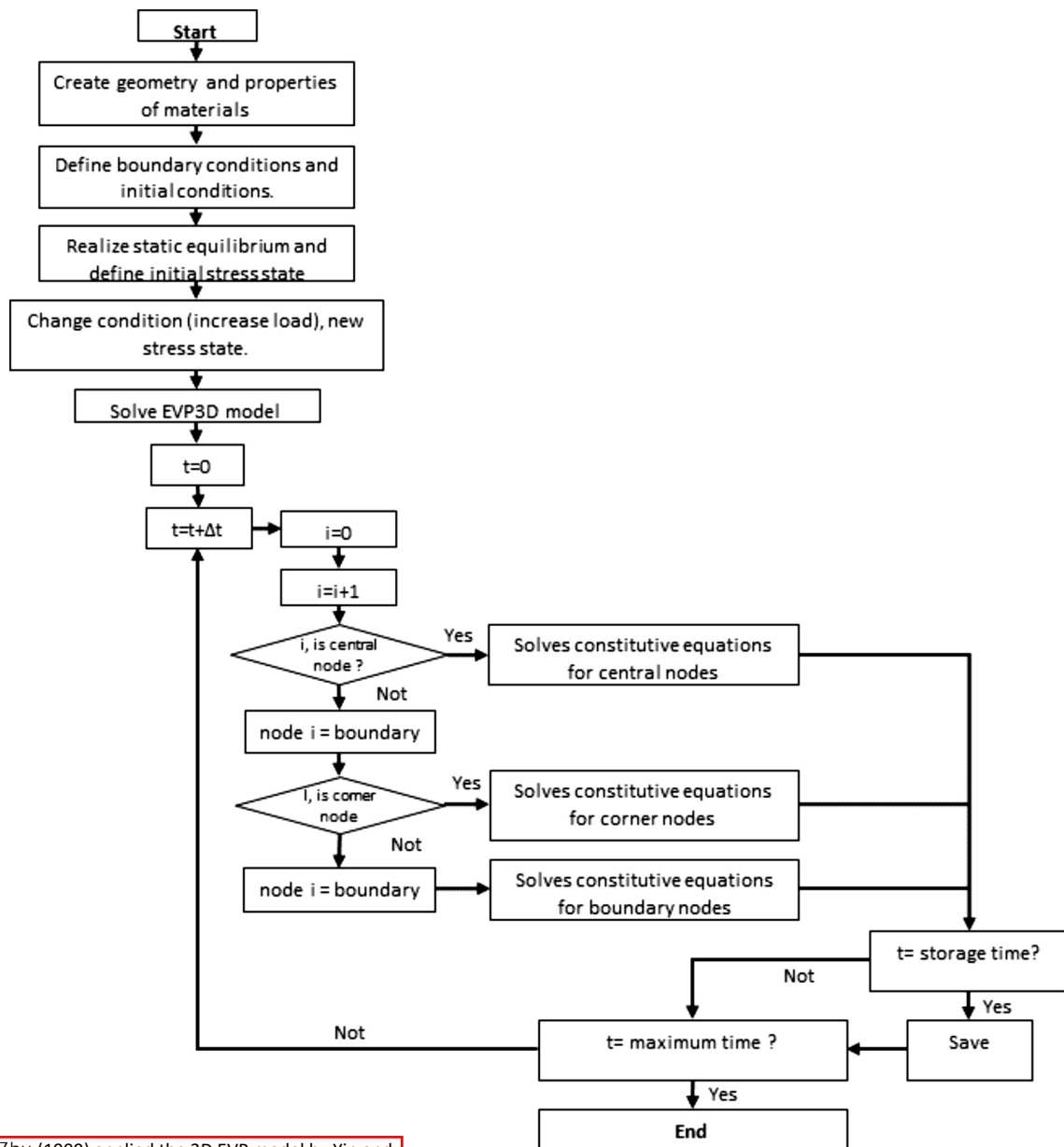
During execution of the EVP model, the system of differential equations that describe the EVP behavior model is solved using the explicit finite difference scheme, which generates the stresses and strains due to the application of external forces.

In Fig. 5, the flowchart for the EVP model code is represented.

4. Validation of the coupled EVP3D model

To calibrate the EVP model in a preliminary work Ossa [15] carried out a comparison between EVP 1D model (which is the basis of the 3D development), Terzaghi's consolidation theory, and measured data obtained from two load increments of a one dimensional consolidation test performed on a specimen of Mexico clay (SS-21-05). Soil parameters used for both simulations are presented in Tables 1 and 2. Fig. 6 shows comparison results and indicate that EVP 1D consolidation settlements predictions (S/Ho) are more reliable than those obtained using 1D conventional theory.

On the other hand, the historical case of the construction of Tarsuit Island was used to verify and validate the results of the algorithm that is implemented in the EVP3D model. This case has been studied by several



Yin and Zhu (1999) applied the 3D EVP model by Yin and Graham (1999) for consolidation modeled of marine soils underneath Tarsuit Island.

5. Flowchart programming EVP3D Model.

Table 1
Soil properties of specimen SS-21-05.

κ/v_o	λ/v_o	ψ/v_o	σ_{ov} (kPa)	ϵ_{zo}'	t_o (min)	k (cm/seg)
0.018	0.29	0.007	158	0	540	$2.5E-08$

researchers, such as Conlin et al. [6] and Yin and Zhu (1999).

Tarsuit Island is located in the Beaufort Sea in the Arctic Ocean between Alaska and northern Canada. This site remains frozen for most

of the year and is considered to be the location of a significant subsea oil reservoir, which has been explored since the 1960s. The island, which is located 60 km off the Canadian coast, was built in 1981. It consists of four sand-filled concrete caissons that rest on a subsea sand berm, and it is 17.5 m high from the foundation to the crown of the berm and 100 m wide. A schematic cross-section of the island is presented in Fig. 7.

The sand berm lies on a soft to slightly rigid marine clay called Zone 1, which is on top of a rigid loamy clay called Zone 2. Zone 2 lies on top of Zone 3, which is composed of frozen soils that are considered to be

Table 2
Parameters of unidimensional consolidation test of specimen SS-21-05.

Incr.	EVP					Terzaghi				
	Ho (m)	$\epsilon_z(z,0)$ (%)	$\sigma_z(z,0)$ (kPa)	$u(i,0) = \Delta \sigma_z$ (kPa)	t (min)	Ho (m)	m_v (m ² /kN)	c_v (m ² /min)	$\Delta \sigma_z$ (kPa)	t (min)
1	0.0189	8.60	200	200	1500	0.0173	$7.5E-04$	$1.5E-06$	200	1500
2	0.0189	26.10	400	400	1500	0.0140	$6.6E-04$	$5.8E-07$	400	1500

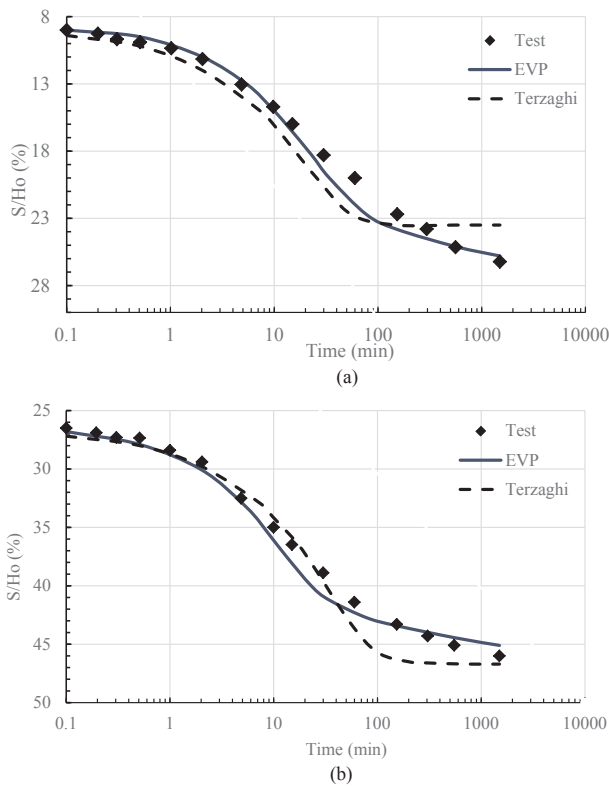


Fig. 6. Calibration 1D EVP model (a) $\Delta\sigma_z = 200$ kPa, (b) $\Delta\sigma_z = 400$ kPa.

rigid and waterproof. Tarsuit Island was instrumented and monitored by Weaver and Berzins (1983), who reported data that were measured at the site until 1985. As part of the instrumentation, two months after completion of construction, an electrical piezometer was installed in Zone 1 two meters from the base of the foundation of the sand berm, with which the evolution of the excess pressure was monitored for 480 days.

4.1. Properties of materials and calculation of initial parameters

The behavioral models for the materials of the island and foundation are different. Linear elastic behavior was assumed for the sand berm and Zone 2, and the EVP3D model was applied for Zone 1. The properties of the materials were determined from data from the piezometer, cone penetration tests (CPTs), index properties, anisotropically consolidated non-drained triaxial tests and odometer tests that were reported by Conlin et al. [6]. The properties of the materials are presented in Tables 3 and 4. Based on the defined behavior model, the values are consistent with those reported by Conlin et al. [6] and Yin and Zhu (1999).

The permeability coefficient k of soils varies with the level of stress and depends directly on the void ratio [22,1,19,20,4,9]. Using accurate information about the permeability of the clay on which Tarsuit Island

Table 3 Properties of the EVP3D model (Zone 1).

Elevation (m)	γ' (kN/m ³)	e_0	K_0	κ/V	λ/V	ϕ'	ν
-21 to -25	8	1.010	0.7	0.0065	0.060	29	0.45
-25 to -26	8	0.950	0.7	0.0056	0.058	29	0.45
-26 to -27	8	0.900	0.7	0.0047	0.052	29	0.45
-27 to -28	8	0.850	0.7	0.0038	0.047	29	0.45
-28 to -29	8	0.790	0.7	0.0028	0.044	29	0.45
-29 to -30	8	0.740	0.7	0.0017	0.037	29	0.45

Table 4 Properties of the linear elastic model (Zone 2 and berm).

Material	γ' (kN/m ³)	E (kPa)	ν	k (m/s)
Zone 2	8	20,000	0.32	1.70E-09
Sand berm	8.1	2000	0.3	-

was built, different permeability conditions were evaluated for this clay stratum based on the ranges reported by Conlin et al. [6] and Yin and Zhu (1999).

To solve the constitutive equations of the EVP3D model, it is necessary to calculate the slopes of the fault envelope (M) in compression and of the moduli K and G according to the following equations:

$$M = \frac{6 \text{sen} \phi'}{(3 - \text{sen} \phi')} \tag{24}$$

$$K = \frac{p}{(\kappa/V)} \tag{25}$$

$$G = 1.5K \frac{(1-2\nu)}{(1 + \nu)} \tag{26}$$

The parameters p'_{mo} and ϵ_{vmo}^{ep} define the point where λ (reference time line) passes (p'_m, ϵ_v) in space [28,29], which is similar to the normal isotropic compression line of the Modified Cam Clay model. The creep parameters ψ/V and t_0 are involved in the EVP3D model. The parameter ψ corresponds to the secondary consolidation coefficient. Based on the EVP 1D model (Yin and Graham, 1990), ψ is approximated as $\psi = C_{\alpha e} / \ln(10)$. The values presented in Table 5 correspond to those reported by Yin and Zhu (1999).

To calculate the initial mean effective stress, p'_{mi} and the initial volumetric strain, ϵ_{vmi} , an overconsolidation ratio $OCR = 3$ was considered for the clay from Zone 1 [6], and the following equations were utilized:

$$p'_{mi} = p'_i + \frac{q_i^2}{p'_i M^2} \tag{27}$$

$$\epsilon_{vmi} = \frac{\lambda}{V} \ln \frac{p'_{mi}}{p'_{mo}} + \left(\frac{\lambda}{V} - \frac{\kappa}{V} \right) \ln OCR \tag{28}$$

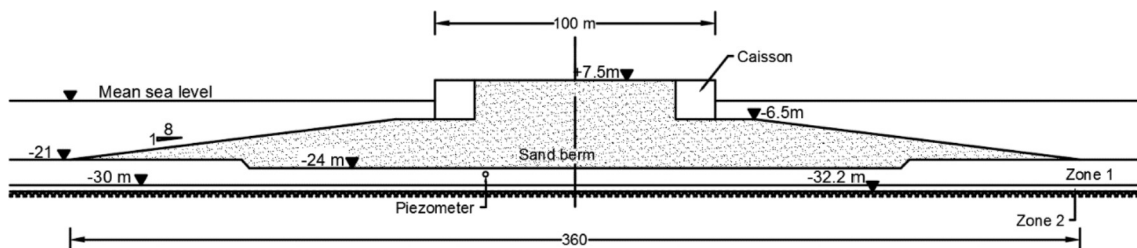


Fig. 7. Schematic cross-section of Tarsuit Island.

Table 5
Parameters of the EVP3D model (Zone 1).

Elevation (m)	P_{m0}' (kPa)	ϵ_{vm0}^{ep}	ψ/V	t_0 (day)	M
-21 to -25	1	0	0.006	1	1.16
-25 to -26	1	0	0.006	1	1.16
-26 to -27	1	0	0.005	1	1.16
-27 to -28	1	0	0.005	1	1.16
-28 to -29	1	0	0.005	1	1.16
-29 to -30	1	0	0.005	1	1.16

4.2. Modeling methodology

The analysis considers the construction process of the island, which lasted for 108 days. The steps proposed by Yin and Zhu (1999) are considered. Stage 0 corresponds to the calculation of the initial stresses. Stages 1 to 5, which have durations of 14 days per stage, correspond to the construction of the sand berm. Stages 6 to 9, which last for a total of 38 days, correspond to the placement of the concrete caissons and the formation of the sand core.

• Geometry and type of analysis

Yin and Zhu (1999) performed a two-dimensional axisymmetric analysis. The algorithm was adapted to this analysis to compare with their results. Fig. 8 shows the analysis model that was constructed in Flac 3D. The variables of the model are in terms of the mean effective stress (p') and the deviatoric stress (q).

The lateral borders are considered to be impermeable and restrict horizontal deformations; only vertical deformations are allowed. This was done to avoid the influence of the lateral borders on the results of the area of interest. The lower boundary of the model is considered to be impermeable because this zone corresponds to frozen soils, and the upper boundary is considered to be a draining boundary.

• Piezometric record

The record of the electric piezometer that was installed in the foundation 60 days after construction of the island at a depth of 2 m and 28 m from the axis of symmetry was used to validate the results. Fig. 9 shows the piezometric record for a period of 485 days.

5. Presentation and analysis of results

The analysis of the stress distribution shows that the total increase in load transmitted to the foundation is 330 kPa, which is equal to the values reported by Conlin et al. [6] and Yin and Zhu (1999).

The variation in the excess pore pressure for different levels of mesh discretization was examined. To corroborate the convergence of the

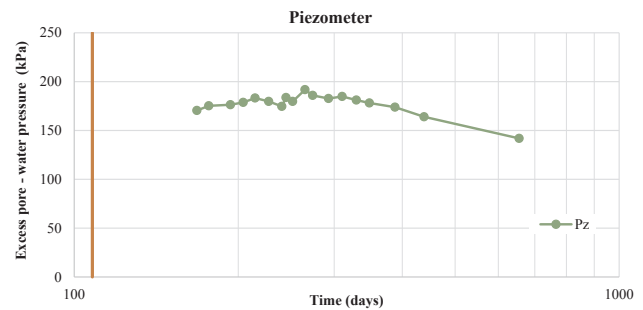


Fig. 9. Piezometric record.

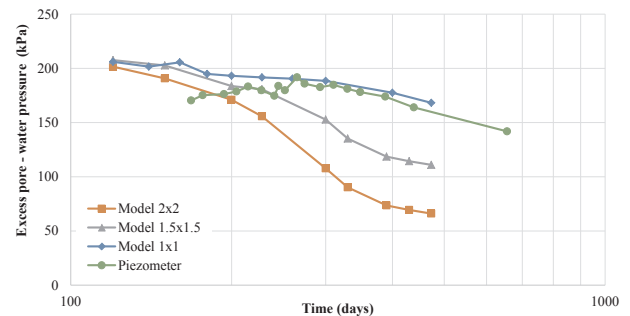


Fig. 10. Model results for different element sizes.

method, mesh geometries with $2\text{ m} \times 2\text{ m}$, $1.5\text{ m} \times 1.5\text{ m}$ and $1\text{ m} \times 1\text{ m}$ elements were analyzed. Fig. 10 compares the results from the three models at the same depth with the electric piezometer record. The results demonstrate that as the size of the elements decreases, the results become more consistent with the piezometric data. The $1\text{ m} \times 1\text{ m}$ model provides a value for the Courant condition that is closest to the reference value; thus, these dimensions are adopted for the subsequent analyses.

During the calibration stage, the EVP3D model was shown to be sensitive to the permeability of the materials. It should be noted that for soft clays, the permeability when the stress is in the preconsolidated range is greater than the permeability in the normally consolidated range because the effective stresses increase over time, and the void ratio decreases (Taylor, 1961). Different authors have reported different permeability values, so it was necessary to perform an inverse parametric analysis. Conlin et al. [6] reported permeability values on the order of $3 \times 10^{-10}\text{ m/s}$ from the surface to the depth of the piezometer and $5 \times 10^{-10}\text{ m/s}$ from the depth of the piezometer to the lower boundary of the compressible stratum. Yin and Zhu (1999) reported a range of permeabilities from $2 \times 10^{-9}\text{ m/s}$ to $5 \times 10^{-11}\text{ m/s}$ for the material in Zone 1.

Fig. 11 shows that using the permeability values proposed by Conlin et al. [6], the response of the model differs from the values of the excess

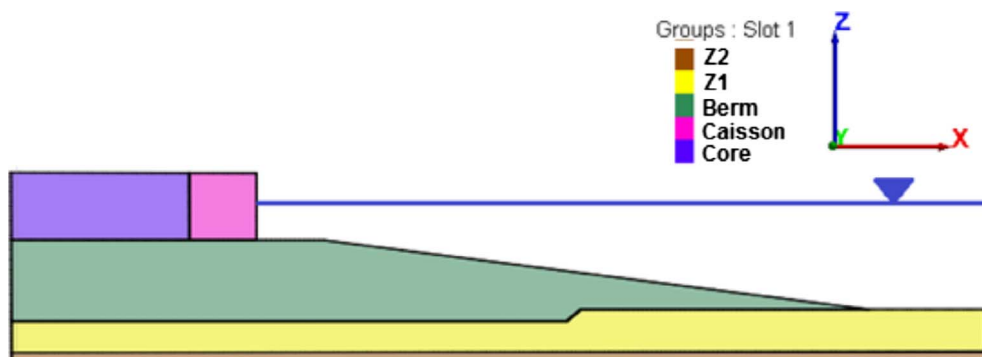


Fig. 8. Geometry of the two-dimensional model.

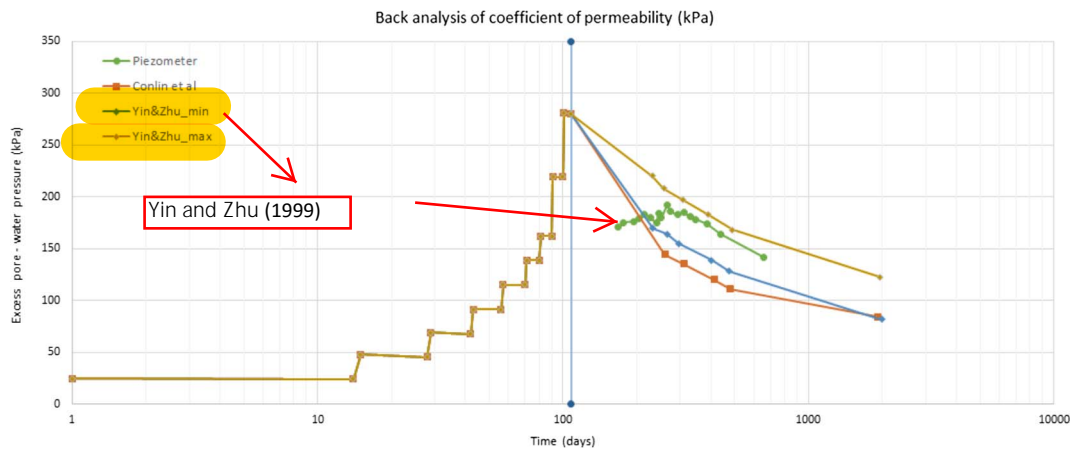


Fig. 11. Effect of the variation of the permeability at piezometer Pz.

pore pressure recorded by the piezometer. The minimum permeability reported by Yin and Zhu (1999) gives values less than those of the piezometric record, and the maximum permeability results in a better approximation of the data.

The values adopted for the permeability (k) based on the parametric analysis are presented in Table 6.

5.1. Excess pore pressure

Fig. 12 shows the variation of the excess pore pressure for an analysis period of 10 years. The variation in the excess pore pressure is monitored at a depth equal to the location of the electric piezometer (2 m below the foundation of the island). Dissipation of the excess pore pressure occurs during each stage of construction, but due to the short duration of each stage, the dissipation is much smaller than the increase in pore pressure at the beginning of the stage. At the end of construction (108 days), the total stress remains constant over time (i.e., there is no variation in the load), and dissipation of the excess pore pressure is observed from this point. The calculated dissipation is a good approximation of that obtained with the piezometric record.

The piezometer record for the first 100 days is characterized by an increase in the excess pore pressure, this may be due to the smearing of the soil surrounding the piezometer tip. It is important to note that in the phase where greater pore pressure dissipation occurred (160 days after completion of construction), and therefore greater deformations in the ground, numerical results reflect a good approximation with the field records. The greatest volumetric changes in the soil occur in this phase of the dissipation process due to consolidation of the soil by the load imposed by the embankment. Fig. 13 shows the predicted variation of the excess pore pressure using isochrones at different times (0 days, 120 days, 1 year, 5 years and 10 years) (see Figs. 14 and 15).

The results indicate that the greatest excess pore pressure occurs at the center of the island, which is the area with the highest load concentrations due to the geometry of the island. The excess pore pressure in the slope area decreases due to the decrease in the transmitted load.

Table 6
Permeability coefficients.

Elevation (m)	k (m/s)
-21 to -25	2.00E-09
-25 to -26	2.00E-09
-26 to -27	5.00E-11
-27 to -28	5.00E-11
-28 to -29	5.00E-11
-29 to -30	5.00E-11

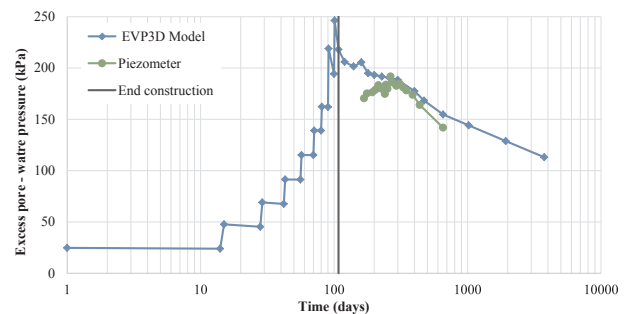


Fig. 12. Comparison of the EVP model results with the piezometric record.

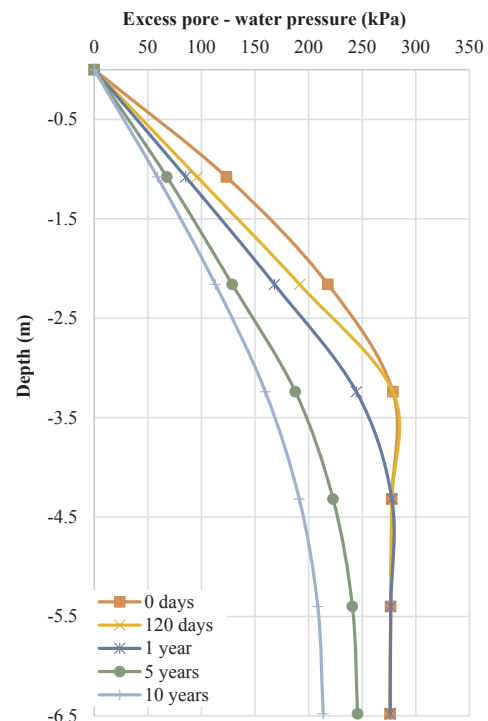


Fig. 13. Variations of the excess pore pressure with depth.

The pore pressure dissipates faster at the periphery than at the center because the excess pore pressure is lower and is located near the upper drainage border. At the end of the analysis period (10 years), the highest values of the excess pore pressure are located at the base of the model near the center, and they approach 200 kPa.

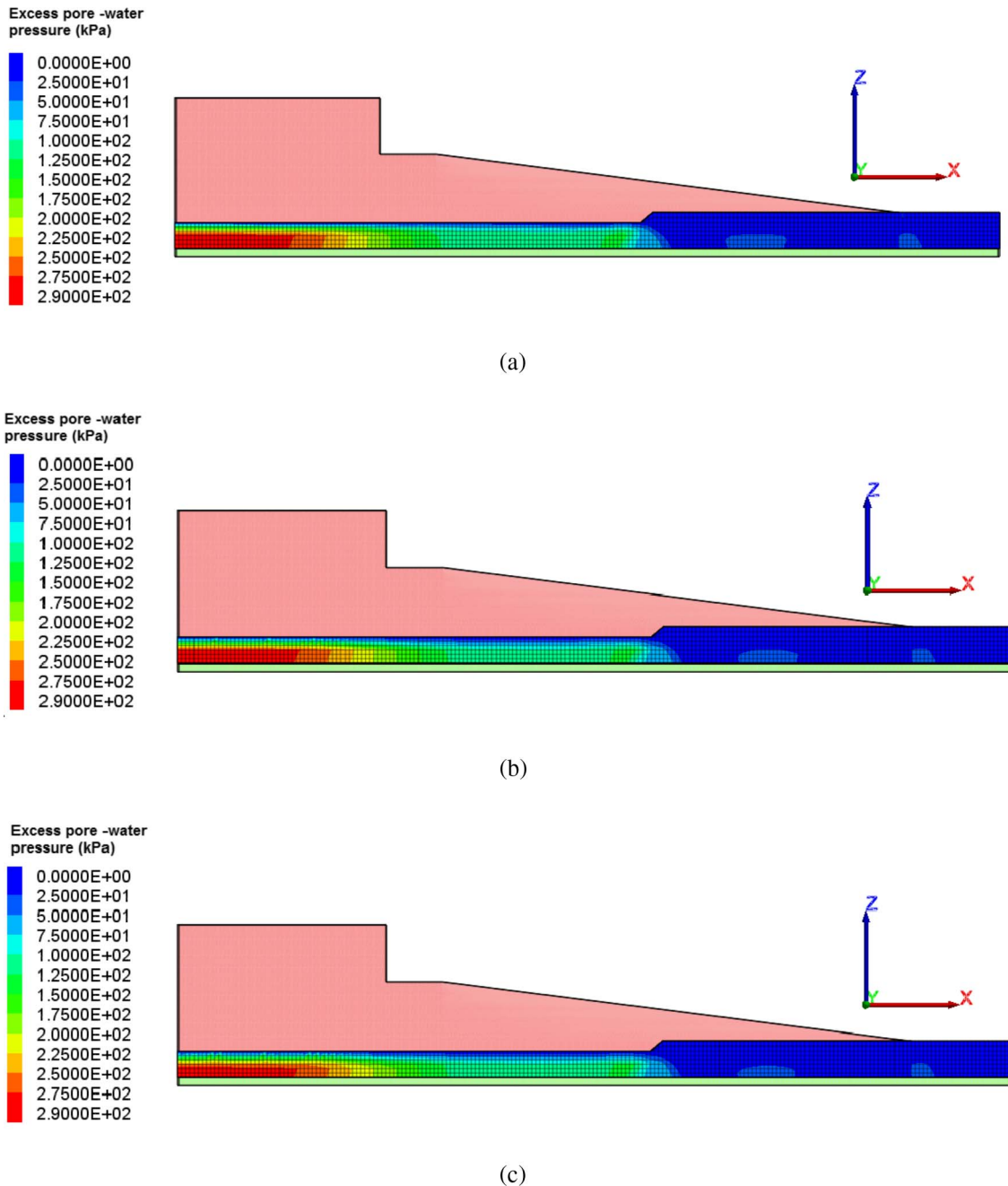


Fig. 14. Excess pore pressure: (a) 0 days, (b) 120 days, (c) 1 year.

5.2. Distribution of effective stresses over time

Fig. 16 shows the isochrones of the vertical effective stress, which show that during the 120 days after the end of construction, the changes in the effective stress are minimal to a depth of approximately 4 m due to the low dissipation of the pore pressure during this period. The vertical effective stress at the base of the compressible stratum (between depths of 4.0 and 6.5 m) does not change until the first year of construction. From 5 to 10 years, the vertical effective stress increases until it reaches 124 kPa at the base of Zone 1.

5.3. Vertical and horizontal displacements

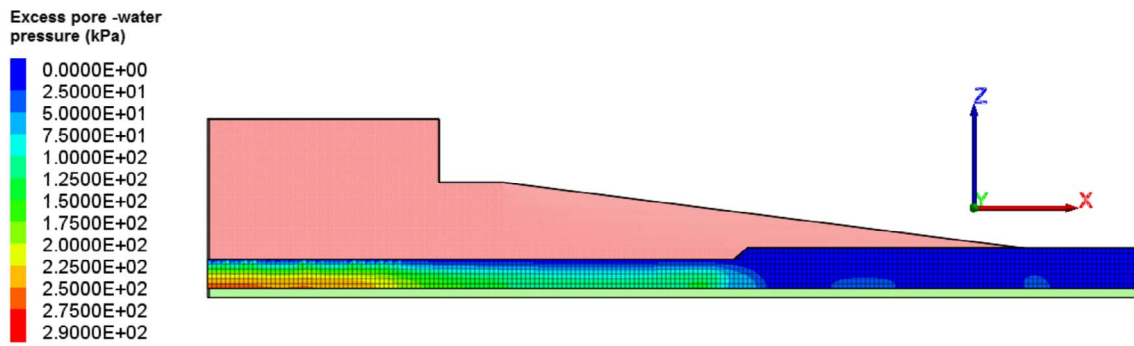
The volumetric (ϵ_v) and deviatoric (ϵ_q) strains are calculated using the constitutive equations of the EVP3D model, and the horizontal and vertical deformations are then determined from the invariants of the

strain tensor [14]. The vertical and horizontal displacements in the upper part of the compressible stratum (Zone 1) are calculated to determine the settlements caused by the construction of the island at 5 and 10 years (Figs. 17 and 18).

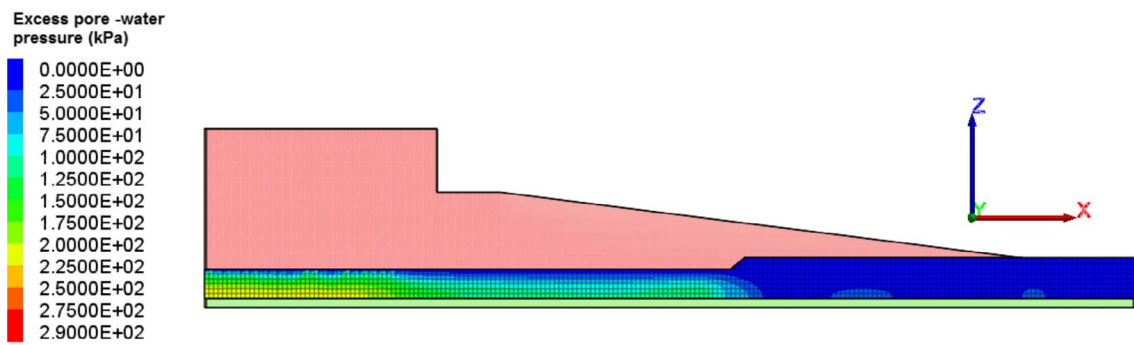
The largest vertical displacements occur in the sand core, which corresponds to the highest part of the island; the vertical displacement reaches 0.4 m after 10 years. The vertical displacements decrease considerably toward the edge of the island. The maximum horizontal displacements are also located in the core area 36 m from the axis of symmetry and reach 0.13 m after 10 years. These results are consistent with those reported by Yin and Zhu (1999).

6. Conclusions

To solve the constitutive equations of the EVP3D model, a coupled consolidation model was proposed and developed based on the general



(a)



(b)

Fig. 15. Excess pore pressure: (a) 5 years, (B) 10 years.

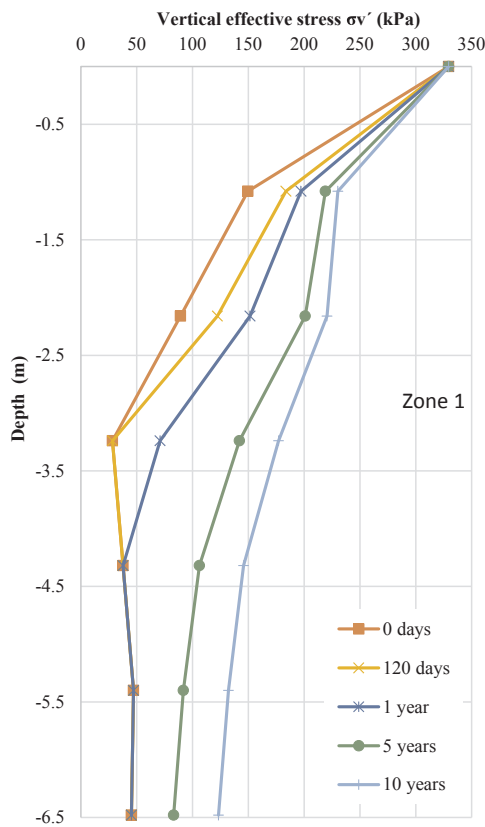


Fig. 16. Variation of the vertical effective stress with depth.

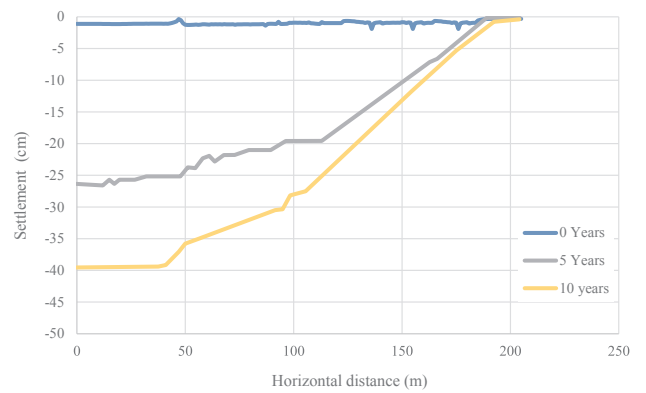


Fig. 17. Vertical displacements measured in the upper part of Zone 1.

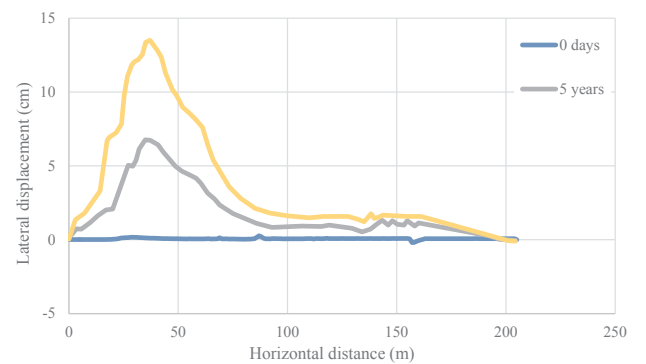


Fig. 18. Horizontal displacements measured in the upper part of Zone 1.

theory of three-dimensional consolidation proposed by Biot [2]. From this model, expressions were obtained to determine the variations of the excess pore pressure, stress state, and volumetric and shear strains of the soil over time.

The programming of the coupled EVP3D model is a new tool for analysis using the finite difference method. Therefore, this model provides an alternative technique for modeling soils that are subject to consolidation processes.

The software Flac3D [12] was used to develop the model using the FISH programming language and the software's programming logic, graphical interface and data storage.

The calibration of the EVP3D program with the case study demonstrated the high sensitivity of the results to the permeabilities used in the consolidation models. Therefore, in future analyses of other problems, appropriate permeabilities must be utilized to ensure that the results accurately represent the behavior of the soil.

Analyses using different levels of mesh discretization were performed in this study. The results showed that the accuracy of the results varies considerably depending on the level of discretization of the problem. In the case study, models with less refined grids provided excess pore pressures that were not consistent with the values obtained from the piezometric data.

The response of the model using the developed algorithm accurately approximated the piezometer data during the dissipation of the pore pressure (i.e., starting 160 days after the construction of the island). The greatest volumetric changes occurred in the soil during this phase due to the increase in the load caused by the construction of the embankment.

Appendix A. Supplementary material

Supplementary data associated with this article can be found, in the online version, at <http://dx.doi.org/10.1016/j.compgeo.2017.11.011>.

References

- [1] Barden L, Berre PL. Consolidation of normally consolidated clay. *J Soil Mech Found Div ASCE* 1965;91(SM5):1–14.
- [2] Biot MA. General theory of three-dimensional consolidation. *J Appl Phys* 1940;12:155–65.
- [3] Bjerrum L. Engineering geology of Norwegian normally consolidated marine clays as related to settlements of buildings, 7th Rankine Lecture. *Geotechnique* 1967;17:83–118.
- [4] Bridle RC, Vaughan PR, Jones HN. Empingham Dam—design, construction and performance. *Proc Instit Civil Eng, Part 1* 1985;78:247–89.
- [5] Casagrande A, Wilson SD. Effect of rate loading on the strength of clays and shales at constant water content. *Geotechnique* 1951;2(3):251–63.
- [6] Conlin BH, Jefferies MG, Maddock WP. An assessment of the Behavior of Foundation Clay at Tarsuit N-44 Caisson Retained Island. In: Proceedings of the 17th offshore technology conference, Houston, Texas, 6–9 May 1985. P. 379–87.
- [7] Courant R, Friedrichs K, Lewy H. On the partial difference equations of mathematical physics. AEC Research and Development Report, NYO-7689, New York: AEC Computing and Applied Mathematics Centre Courant Institute of mathematical Sciences; September 1956.
- [8] Desai CS, Zhang D. Viscoplastic model for geological materials with generalized flow rule. *Int J Numer Anal Meth Geomech* 1987;11:603–20.
- [9] Fox PJ. Analysis of hydraulic gradient effects for laboratory hydraulic conductivity testing. *Geotech Test J* 1996;19(2):181–90.
- [10] Gonzalez R, Ossa A, Ovando SE. Prediction of settlements due to regional subsidence in the zone of the old lake of Texcoco. XV Panamerican conference of soil mechanics and geotechnical engineering, Argentina; 2015 [in Spanish].
- [11] Graham J, Crooks JHA, Bell AL. Time effects on stress-strain behavior of natural soft clay. *Geotechnique* 1983;33(3):327–40.
- [12] Itasca Consulting Group INC. Flac 3D User's Guide. Fourth Edition, USA; 2009.
- [13] Leroueil S, Kabbaj M, Tavenas F, Bouchard R. Stress-strain-strain rate relation for compressibility of sensitive natural clays. *Geotechnique* 1985;35(2):159–80.
- [14] Malvern LE. Introduction to the mechanics of a continuous medium. New Jersey: Prentice Hall; 1969.
- [15] Ossa A. Modelo elastoviscoplastico (EVP) para el estudio de la consolidación unidimensional de los suelos. Master thesis. Universidad Nacional Autónoma de México. UNAM; 2004.
- [16] Ovando SE. Creep Effects on the clay from Mexico Basin. In: Proceedings of the international conference on creep and deformation characteristics in geomaterials, Gothenburg, Sweden; 2015.
- [17] Perzyna P. Fundamental problems in viscoplasticity. *Adv Appl Mech* 1966;9:244–368.
- [18] Roscoe KH, Burland JB. On the generalised stress-strain behaviour of wet clay. In: Heyman J, Leckie FP, editors. Engineering plasticity. New York: Cambridge University Press; 1968. p. 535–609.
- [19] Samarasinghe AM, Huang YH, Drnevich VP. Permeability and consolidation of normally consolidated soils. *J Geotech Eng Div, ASCE* 1982;108(GT6):835–50.
- [20] Tavenas F, Jean P, Leblond P, Leroueil S. The permeability of natural soft clays. Part II: Permeability characteristics. *Can Geotech J* 1983;20:645–60.
- [21] Tavenas F, Leroueil S, LaRochelle P, Roy M. Creep behavior of an undisturbed lightly overconsolidated clay. *Can Geotech J* 1978;15:402–23.
- [22] Taylor DW. Fundamentals of Soil Mechanics. New York: John Wiley & Sons Inc.; 1948.
- [23] Wehnert, Neher. An evaluation of soft soil models based on trial embankments. In: Computer methods and advances in geomechanics: Proceedings of the 10th international conference on computer methods and advances in geomechanics; 2000.
- [24] Wood DM. Geotechnical modelling. Londres, Inglaterra: Cambridge University Press; 2004.
- [25] Yin J-H, Graham J. Viscous-elastic-plastic modelling of one-dimensional time-dependent behaviour of clays. *Can Geotechn J* 1989;26:199–209.
- [26] Yin J-H, Graham J. Equivalent times and one-dimensional elastic visco-plastic modelling of time-dependent stress-strain behaviour of clays. *Can Geotech J* 1994;31:42–52.
- [27] Yin JH, Graham J. Elastic visco-plastic modelling of one dimensional consolidation. *Geotechnique* 1996;46(3):515–27.
- [28] Yin JH, Graham J. Elastic viscoplastic consolidation modelling and interpretation of pore water pressure responses in clay underneath Tarsuit Island. *Can Geotech J* 1999;36(1):708–17.
- [29] Yin JH, Graham J. Elastic viscoplastic modelling of the time dependent stress-strain behavior of soils. *Can Geotech J* 1999;36(1):736–45.